Real-Time Incident-Responsive System for Corridor Control: Modeling Framework and Preliminary Results

GANG-LEN CHANG, JIFENG WU, AND HENRY LIEU

An integrated optimal control model has been formulated to address the dynamic freeway diversion control process. An effective and efficient approach is developed for simultaneously solving diversion control measures, including on-ramp metering rates, off-ramp diversion rates, and green/Cycle ratios for traffic signals on a real-time basis. By approximating the flow-density relation with a two-segment linear function, the nonlinear optimal control problem can be simplified into a set of piecewise linear programming models and solved with the proposed successive linear programming algorithm. Consequently, an effective on-line feedback approach has been developed for integrated real-time corridor control. Preliminary simulation results with INTRAS for a sample network have demonstrated the merits of the proposed model and algorithm.

Real-time traffic control for freeway corridors has been the subject of increasing research in recent years because of nonrecurrent traffic congestion, especially that due to incidents. For a typical freeway corridor system consisting of a mainline freeway, a parallel surface street, and ramps, an integrated traffic control scheme should include three basic elements: (*a*) on-ramp metering, (*b*) off-ramp diversion, and (*c*) signal timing at surface street intersections. Another possible control measure, segmentwide speed limitation, has also been studied by European researchers (*1,2*). However, this measure appears impractical and is not recommended in the United States.

Although ramp metering and signal timing at street intersections have received much attention both in theoretical research and in real-world applications, relatively few attempts at real-time diversion control have been made. In fact, during a severe freeway incident, on-ramp metering usually is not adequate to relieve congestion effectively. Diverting some traffic to the parallel surface street to make full use of available corridor capacity will be necessary. However, to determine the optimal time-varying diversion flow rates when an incident is detected is a challenging task. Effective integration of on-ramp metering, off-ramp guidance, and signals on surface streets will be essential to ensure successful operation of the entire freeway corridor.

A review of the literature yielded some studies on corridor control. Cremer and Schoof (*1*) formulated a comprehensive corridor control model and proposed a heuristic on-line control algorithm on the basis of off-line solutions. Chang et al. (*3*) developed a prototype model for dynamic system-optimal control that provides coordinated operation between mainline and surface streets, but off-ramp flow diversion was not treated as a control measure. Earlier studies conducted by Gartner and Reiss (*4*) and Reiss et al. (*5–7*) made significant contributions to this topic, applying a creative multilevel control structure; however, no specific on-line diversion strategies at off-ramps were investigated. Other studies conducted by Goldstain and Kumar (*8*), Papageorgiou (*9,10*), Papageorgiou et al. (*11*), and Payne et al. (*12*) addressed only mainline freeway control.

Evidently, all three corridor control measures should be integrated in formulating corridor traffic models to achieve an optimal control. At the same time, an efficient solution algorithm must be designed for real-time applications. Only Cremer and Schoof (*1*) have developed an integrated optimal control model that includes all control variables. However, their proposed model is very difficult to solve, because it turns out to be a large-scale, nonlinear, mixed integer optimization problem, and thus real-time applications are precluded. As a result, their proposed solution algorithm is not able to handle all the control variables simultaneously. Hence, the model has to resort to a two-stage optimization procedure in which the upper level is made for route diversion and the lower level for ramp metering, speed limitation, and signaling of surface street intersections.

The need to make a decision in real time may dictate the selection of traffic models and an optimization algorithm. A certain trade-off between computational effort and an affordable level of modeling details is inevitable. Whereas analytical linearization techniques can be used to tackle nonlinear models, such algorithms generally are not efficient because of the intensive computation requirements. Hence, development of an effective algorithm is also at the core of an on-line diversion control system.

The purpose of this research is to formulate a set of linear or piecewise linear models that address all issues in an integrated incident-responsive corridor control system. The framework of a real-time corridor control system is outlined in the next section. By adopting a two-segment linear flow-density model, a set of piecewise linear optimal control models was developed, including on-ramp metering rates, off-ramp diversion rates, and green/Cycle (g/C) ratios for surface street signals. An efficient solution algorithm was developed that makes the proposed diversion control model sufficiently fast for use in real-time applications. Finally, an illustrative example conducted with a corridor simulation model (INTRAS) is outlined to demonstrate the efficacy of the proposed approach.

SYSTEM DESCRIPTION

Consider a typical freeway corridor, consisting of a unidirectional freeway segment, a parallel surface street/arterial, and a number of on- and off-ramps. The entire corridor is divided into N small segments, each having the same topological structure as shown in Figure 1 and containing only one pair of on- and off-ramps and one

G-L. Chang and J. Wu, Department of Civil Engineering, University of Maryland, College Park, Md. 20742. H. Lieu, IVHS Division, HSR-10, FHWA, 6300 Georgetown Pike, McLean, Va. 22101.

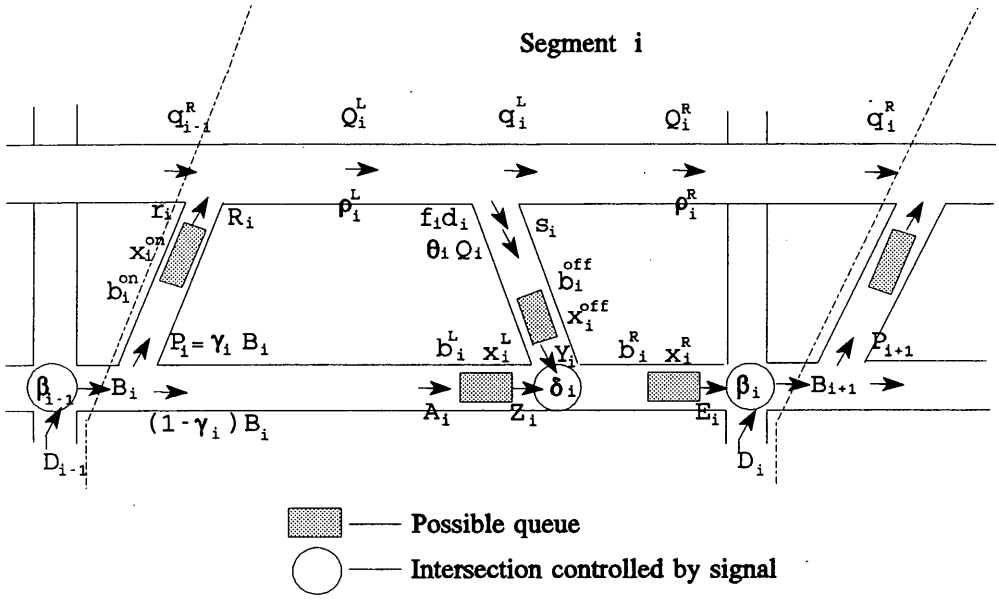

FIGURE 1 Arguments of Segment *i* and their notations.

crossing street. The off-ramp naturally divides the whole segment into two subsegments, the left part and the right part. Whereas each parallel street segment is divided into three subsections, it is assumed that (*a*) each on-ramp is close to its upstream surface street intersection and the distance between them is negligible from the congestion control perspective and (*b*) the distance between each street intersection and its adjacent upstream off-ramp intersection is short so that the link free flow time is negligible (but its waiting time may be significant because of limited street storage). Hence, for each surface street segment, the analysis of traffic dynamics may be focused mainly on two aspects: queuing at its downstream intersections and flow transition from the upstream to the downstream.

As indicated previously, metering at the on-ramps may not be sufficient if the incident is severe. Diverting freeway traffic via off-ramps may be necessary. However, the fraction of traffic to be diverted needs to be determined so that the prespecified system objective (e.g., corridor throughput) can be optimized. At the same time, signal timing at street intersections should be responsive to the diverting traffic to best serve traffic in the entire corridor. Hence, in the proposed model, we focus on formulating the interactions between those key control elements. All continuous variables are discretized into small equal intervals for analyses. The duration of each time interval is denoted as T. Notation and definitions of all relevant variables and parameters used hereafter are given in Table 1. With these defined variables, the principal issue is to solve the optimal on-line control strategies $\{R_i(k), d_i(k), \delta_i(k), \beta_i(k)\}$ according to traffic surveillance data and all other available information.

DYNAMIC TRAFFIC MODELS

Mainline Traffic Dynamics

If an equilibrium flow-density relationship prevails for each segment i, the traffic state on a segment can be represented with the mean segment density. A dynamic density evolution equation, according to the flow conservation law, can be formulated as follows:

$$\rho_i^L(k) = \rho_i^L(k-1) + \frac{T}{L_i^L l_i^L}[q_{i-1}^R(k) + e_i(k)R_i(k) - f_i(k)d_i(k) - \theta_i(k)Q_i^L(k) - q_i^L(k)] \qquad 1 \le i \le N \tag{1}$$

$$\rho_i^R(k) = \rho_i^R(k-1) + \frac{T}{L_i^R l_i^R}[q_i^L(k) - q_i^R(k)] \qquad 1 \le i \le N \tag{2}$$

where $e_i(k)R_i(k)$ and $f_i(k)d_i(k)$ express the actual flow rates at the entry on-ramp and exit off-ramp, respectively, of mainline Segment i, with $e_i(k)$ and $f_i(k)$ representing the actual system compliance parameters to the control measures $R_i(k)$ and $d_i(k)$. It is notable that $\theta_i(k)Q_i^L(k)$ is the regular flow rate exiting at off-ramp i, whereas $f_i(k)d_i(k)$ is the additional flow rate that needs to be diverted.

To capture the dynamic interrelations between adjacent segment flows, the transition flow between adjacent segments is taken as the average of the two adjacent segment boundary flows. More specifically, it is given by

$$q_i^L(k) = \frac{1}{2}\{[1 - \theta_i(k)]\,Q_i^L(k) - f_i(k)\,d_i(k) + Q_i^R(k)\} \qquad 1 \le i \le N \tag{3}$$

$$q_i^R(k) = \frac{1}{2}[Q_i^R(k) + Q_{i+1}^L(k) - e_{i+1}(k)R_{i+1}(k)] \qquad 1 \le i \le N-1 \tag{4a}$$

$$q_N^R(k) = Q_N^R(k) \tag{4b}$$

where Equation 4b, describing the mainline downstream boundary flow, is a special case.

Generally, the density dynamic equations are nonlinear because flow rate, $Q_i(k)$, is usually a nonlinear function of density, $\rho_i(k)$. That limits most of the equations' networkwide applications to off-line cases or to small networks because of considerable compu-

TABLE 1 Definition of System Variables

Network geometric and physical data	
L_i^L:	physical length (miles) of the left-section of freeway Segment i
l_i^L:	number of lanes of the left-section of freeway Segment i
L_i^R:	physical length (miles) of the right-section of freeway Segment i
l_i^R:	number of lanes in the right-section of freeway Segment i
L_i^s:	physical length (miles) of street Segment i
u_i^L, v_i^L:	parameters of flow-density relationship for the left section of freeway Segment i
u_i^R, v_i^R:	parameters of flow-density relationship for the right section of freeway Segment i
ρ^{cr}:	critical density (vehicle/lane/mile) at which freeway flow reaches its maximum
ρ^{max}:	jam density (vehicle/lane/mile) of the freeway
V_i:	normal flow speed (mph) of street Segment i
R_i^{max}:	maximum metering rate (mph) for On-ramp i
R_i^{min}:	minimum metering rate (mph) for On-ramp i
b_i^{on}:	maximum number of queue vehicles permitted on On-ramp i
b_i^{off}:	maximum number of queue vehicles permitted on Off-ramp i
b_i^R:	maximum number of queue vehicles permitted on the right section of arterial street Segment i
b_i^L:	maximum number of queue vehicles permitted on the left section of arterial street Segment i
C_i^{off}:	queue discharge rate (vehicle/green-hour) of Off-ramp i
C_i^R:	queue discharge rate (vehicle/green-hour) at the crossing intersection of arterial street Segment i
C_i^L:	queue discharge rate (vehicle/green-hour) at the off-ramp intersection of arterial street Segment i
Dynamic traffic demand	
$q_0^R(k)$:	flow rate (vph) entering the upstream end of freeway Segment 1 during interval k
$B_1(k)$:	flow rate (vph) entering the upstream end of street Segment 1 during interval k
$D_i(k)$:	flow rate (vph) approaching the corridor from the crossing street of segment i during interval k
$\theta_i(k)$:	proportion of traffic leaving freeway via off-ramp i (not including the diverted portion) during interval k
$\lambda_i(k)$:	the fraction of through traffic of $D_i(k)$
Incident data	
$\sigma_i^L(k)$:	capacity reduction factor due to an incident on the left section of freeway segment i, and $[1-\sigma_i^L(k)]100\%$ representing the reduced percentage of capacity
$\sigma_i^R(k)$:	capacity reduction factor due to an incident on the right section of freeway segment i, and $[1-\sigma_i^R(k)]100\%$ representing the reduced percentage of capacity

(*continued on next page*)

tational complexity. However, if a linear or piecewise linear $Q_i(k) \sim \rho_i(k)$ approximation is acceptable, it is obvious that the dynamic density equations (Equations 1 and 2) and the flow-density relations (Equations 3 and 4) become linear or piecewise linear, and the computational burden associated with the nonlinearity can be substantially alleviated. In fact, a two-segment linear flow-density model provides a good fit for freeway traffic operations according to recent research results (*13,14*). Figure 2 shows such a two-segment linear function, where ρ^{cr} represents the critical density at which the flow rate reaches its maximum and ρ^{max} is the jam density value.

Now suppose a two-segment linear flow-density function has been calibrated for each freeway Segment *i*:

$$Q_i^L(k) = [v_i^L(\rho) + u_i^L(\rho) \cdot \rho_i^L(k)]\sigma_i^L(k) \qquad 1 \le i \le N \tag{5}$$

$$Q_i^R(k) = [v_i^R(\rho) + u_i^R(\rho) \cdot \rho_i^R(k)]\sigma_i^R(k) \qquad 1 \le i \le N \tag{6}$$

TABLE 1 (*continued*)

Traffic Volumes (average flow rates in vph)

$q_i^L(k)$: flow rate from left section to right section of freeway Segment i during interval k

$q_i^R(k)$: flow rate from freeway Segment i to Segment i+1 during interval k

$Q_i^L(k)$: flow rate of left section of freeway Segment i during interval k

$Q_i^R(k)$: flow rate of right Section of freeway Segment i during interval k

$r_i(k)$: flow rate entering the freeway from on-ramp i during interval k

$s_i(k)$: flow rate (involving diverted traffic) leaving the freeway via off-ramp i during interval k

$B_i(k)$: flow rate entering upstream of street Segment i during interval k

$A_i(k)$: flow rate on the left section of street Segment i approaching the off-ramp junction during interval k

$Z_i(k)$: flow rate discharging from the off-ramp intersection on street Segment i during interval k

$E_i(k)$: flow rate discharging from downstream intersection of street Segment i during interval k

$Y_i(k)$: flow rate discharging from downstream Off-ramp i and merging into arterial street during interval k

$P_i(k)$: mean flow rate entering on-ramp i from the arterial street during interval k

System Parameters

$\gamma_i(k)$: proportion of the arterial street traffic entering on-ramp i during interval k

$e_i(k)$: ratio of actual flow rate entering the freeway to the metering rate for on-ramp i during interval k

$f_i(k)$: ratio of actual diverting flow rate to the calculated diversion rate for off-ramp i during interval k

$\alpha_i(k)$: platoon dispersion parameter of street segment i

$\eta_i(k)$: fraction of through traffic from street segment i to street segment i+1

$t_i(k)$: mean travel time to traverse the left section of street segment i during interval k

Control Variables to Be Solved

$R_i(k)$: metering flow rate (vph) for On-ramp i during interval k

$d_i(k)$: flow rate (vph) for freeway diversion at off-ramp i not including normal turning traffic during interval k

$\delta_i(k)$: g/c ratio for signal timing at off-ramp intersection i for the arterial traffic during interval k

$\beta_i(k)$: g/c ratio for signal timing at crossing street intersection i for the arterial traffic during interval k

State Variables

$\rho_i^L(k)$: mean density (vehicle/lane/mile) of the left section of freeway Segment i during interval k

$\rho_i^R(k)$: mean density (vehicle/lane/mile) of the right section of freeway Segment i during interval k

$x_i^{on}(k)$: average number of vehicles on on-ramp i during interval k

$x_i^{off}(k)$: average number of vehicles on off-ramp i during interval k

$x_i^R(k)$: average number of vehicles on the right section of street Segment i during interval k

$x_i^L(k)$: average number of queuing vehicles on the left section of street Segment i during interval k

where each of the coefficients $v_i^L(\rho)$, $u_i^L(\rho)$ and $v_i^R(\rho)$, $u_i^R(\rho)$ take two different values, depending on which regime the density values fall into, and $\sigma_i^L(k)$ and $\sigma_i^R(k)$ represent the corresponding capacity reduction factors due to the incident. For those segments not affected by the incident, parameters σ_i^L and σ_i^R naturally equal 1. Thus, Equations 1 through 6 constitute a set of piecewise linear models for the mainline segment density dynamics.

Ramp Traffic Dynamics

To simplify the presentation, the lengths of all the ramp links are assumed to be relatively short, and thus the traffic state at ramps can be represented with its dynamic queuing length evolution. If the travel time on any ramp is not negligible, a flow transition equation using Robertson's platoon dispersion model (*15*) can be employed

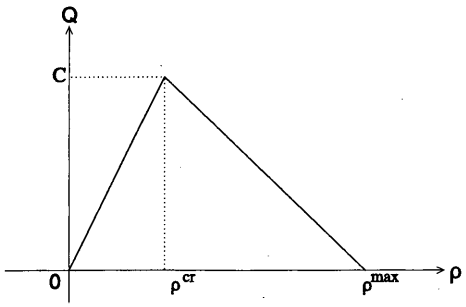

FIGURE 2 Two-segment linear flow-density model.

to capture the traffic variation as used for arterial segments. With such simplifications, the on-ramp queuing length dynamics can be formulated as follows on the basis of the conservation law:

$$x_i^{on}(k) = x_i^{on}(k-1) + [\gamma_i(k)B_i(k) - e_i(k)R_i(k)]T \qquad 1 \le i \le N \tag{7}$$

where $B_i(k)$ is the oncoming flow rate at the upstream end of surface street segment i and $\gamma_i(k)$ is the decimal proportion of $B_i(k)$.

Similarly, the queuing length dynamics for off-ramps can be given by

$$x_i^{off}(k) = x_i^{off}(k-1) + [f_i(k)\,d_i(k) + \theta_i(k)Q_i^L(k) - Y_i(k)]T \qquad 1 \le i \le N \tag{8}$$

The downstream off-ramp discharging flow, $Y_i(k)$, is affected by the signal timing at its downstream junction with the arterial. Assuming that a two-phase signal timing is applied for each off-ramp intersection and each crossing street intersection, the g/C ratios assignment $\{\delta_i(k)\}$ is the only control variable to be optimized. Given an off-ramp capacity, the average off-ramp discharging flow can be computed by

$$Y_i(k) = \min\left\{[1-\delta_i(k)]C_i^{off}, \frac{x_i^{off}(k-1) + [f_i(k)\,d_i(k) + \theta_i(k)Q_i^L(k)]\,T}{T}\right\} \qquad 1 \le i \le N \tag{9}$$

where the last item on the right-hand side expresses the average flow rate, if the queue on the off-ramp i can be cleared at the end of time interval k.

Surface Street Traffic Models

For each surface street segment i, the queues due to incidents shall be considered at both the segment's downstream off-ramp junction and the crossing street intersection. We assume that all intersections are under two-phase signal control. The g/C ratios for the arterial traffic, $1-\delta_i(k)$ and $\beta_i(k)$, are thus the two key control parameters to be optimized.

For the left-hand-side section of arterial segment i, it can be seen that the downstream flow $A_i(k)$, approaching the off-ramp junction, is determined to some extent by the upstream flow rate $[1-\gamma_i(k')]B_i(k')$ over the previous time interval k'. One of the most commonly used formulations for such a relation is the following platoon dispersion model (*15,16*):

$$A_i(k) = [1-\alpha_i(k)]B_i'(k) + \alpha_i(k)A_i(k-1) \qquad 1 \le i \le N \tag{10}$$

where

$$B_i'(k) = \{1-\gamma_i[k-t_i'(k)]B_i[k-t_i'(k)]\} \qquad 1 \le i \le N \tag{11}$$

and $t_i'(k)$ is the closest integer to the value $0.8t_i(k)/T$; $t_i(k)$ is the average travel time required for traversing surface street segment i when joining the queue within interval k; $\alpha_i(k)$ is the dynamic smoothing parameter.

With Equations 10 and 11, we can establish the interrelation between upstream and downstream flows on arterial segment i.

Similar to Equations 7 and 8, the queuing length dynamics for both possible downstream queues can be modeled as follows:

$$x_i^L(k) = x_i^L(k-1) + [A_i(k) - Z_i(k)]T \qquad 1 \le i \le N \tag{12}$$

$$x_i^R(k) = x_i^R(k-1) + [Z_i(k) + Y_i(k) - E_i(k)]T \qquad 1 \le i \le N \tag{13}$$

In the same fashion as Equation 9, discharging flows at the downstream end can be expressed with the following:

$$Z_i(k) = \min\left[\delta_i(k)C_i^L, \frac{x_i^L(k-1) + A_i(k)T}{T}\right] \qquad 1 \le i \le N \tag{14}$$

$$E_i(k) = \min\left\{\beta_i(k)C_i^R, \frac{x_i^R(k-1) + [Z_i(k) + Y_i(k)T}{T}\right\} \qquad 1 \le i \le N \tag{15}$$

Finally, the interactions between surface street flows in neighboring segments can be established through the following flow conservation relation at intersections:

$$B_{i+1}(k) = D_i(k)[1-\lambda_i(k)][1-\beta_i(k)] + \eta_i(k)E_i(k) \qquad 1 \le i \le N \tag{16}$$

where

$D_i(k)[1-\lambda_i(k)]$ = demand flow rate entering the corridor from the crossing street i during interval k,
$[1-\beta_i(k)]$ = g/C ratio for crossing street i, and
$\eta_i(k)$ = proportion of through traffic at the downstream end of surface street segment i during interval k.

FRAMEWORK OF REAL-TIME CONTROL APPROACH

Dynamic System Evolution

Using the notation defined previously, the dynamic state of the entire corridor (see Figure 3) at any time interval can be represented as

$$W(k) = F[W(k-1), C(k), G(k), H(k)]$$

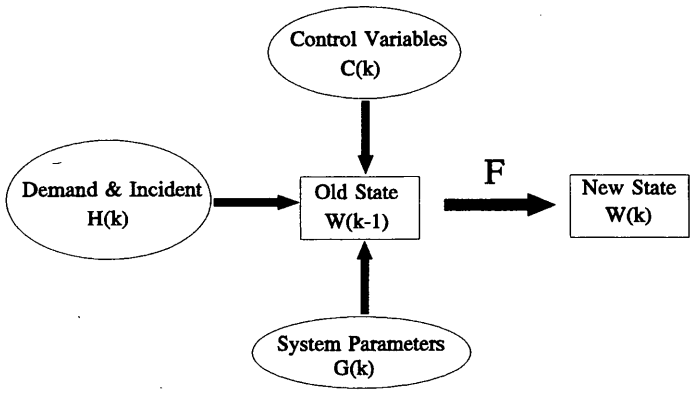

FIGURE 3 Dynamic traffic state evolution mechanism.

where

$W(k) \equiv \{\rho_i^L(k), \rho_i^R(k), x_i^{on}(k), x_i^{off}(k), x_i^L(k), x_i^R(k) \mid \text{for all } i\}$ represents the traffic state at interval k,

$C(k) \equiv \{R_i(k), d_i(k), \delta_i(k), \beta_i(k) \mid \text{for all } i\}$ denotes all control measures to be optimized,

$G(k) \equiv \{\gamma_i(k), e_i(k), f_i(k), \alpha_i(k), \eta_i(k), t_i(k) \mid \text{for all } i\}$ denotes the time-dependent system model parameters,

$H(k) \equiv \{D_i(k), \lambda_i(k), \theta_i(k), \sigma_i^L(k), \sigma_i^R(k) \mid \text{for all } i\}$ includes both the real time travel demand pattern and incident information; and

F = function determined by Equations 1 through 16.

The interrelations between principal modules as well as the control logic are shown in Figure 4. Key functions of each principal module are presented.

Optimal Control Model

The real-time incident-responsive control problem is to determine optimal control measures $C(k)$ (i.e., on-ramp metering rates, off-ramp diversion flow rates, and g/C ratios for surface street signals) for time interval k and its subsequent intervals, at the beginning of each time interval k, with the given time-varying travel demand pattern and incident information $\{H(t)\}$.

Depending on an operation agency's major concern, one may choose different control objectives, for example, to minimize the total travel time, waiting time, delay, vehicle-hours, vehicle-miles, or pollutant emissions. In this study, we select the total corridor throughput as the only measure of effectiveness, because it is the primary concern after an incident. The total corridor throughput includes vehicles exiting the corridor at surface street intersections and at the last control segment of both the freeway and the arterial. A mathematical expression of the corridor throughput is given by

$$\sum_k \left(\sum_{i=1}^{N} \{[1 - \eta_i(k)]E_i(k) + [1 - \beta_i(k)]\lambda_i(k) D_i(k)\}T + [q_N^R(k) + B_{N+1}(k)]T \right) \quad (17)$$

Assuming that all the related parameters are available, an optimal control model can then be calibrated and executed to maximize the objective function, subject to the dynamic constraints (Equations 1 through 16) and the boundary constraints given in Equations 18 through 25. Equation 18 represents metering rates, Equation 19 represents diverting flows, Equations 20 through 23 represent queuing lengths, and Equations 24 and 25 represent g/C ratios in signal timing.

$$R_i^{min} \le R_i(k) \le R_i^{max} \qquad 1 \le i \le N \quad (18)$$

$$0 \le d_i(k) \le C_i^{off} - \theta_i(k) Q_i^L(k) \qquad 1 \le i \le N \quad (19)$$

$$0 \le x_i^{on}(k) \le b_i^{on} \qquad 1 \le i \le N \quad (20)$$

$$0 \le x_i^{off}(k) \le b_i^{off} \qquad 1 \le i \le N \quad (21)$$

$$0 \le x_i^L(k) \le b_i^L \qquad 1 \le i \le N \quad (22)$$

$$0 \le x_i^R(k) \le b_i^R \qquad 1 \le i \le N \quad (23)$$

$$0 \le \delta_i(k) \le 1 \qquad 1 \le i \le N \quad (24)$$

$$0 \le \beta_i(k) \le 1 \qquad 1 \le i \le N \quad (25)$$

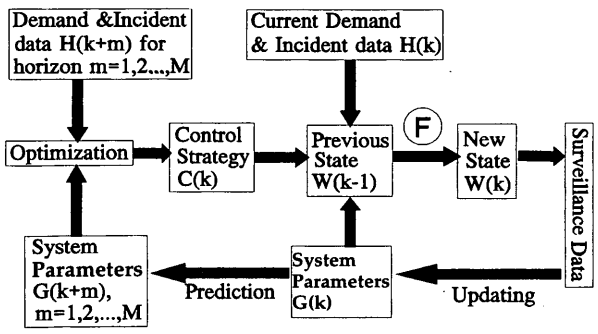

FIGURE 4 Flowchart of real-time corridor control logic.

Because the proposed model has addressed all essential aspects of corridor control, theoretically one can extend the optimal time horizon to the entire control period of interest. However, because of the computing burden and the increasing uncertainty for predicted demands, we recommend that optimal control be extended at a short

time interval preceded by a commonly used rolling time horizon method (*17–19*).

Parameter Updating and Prediction

Under nonrecurrent freeway congestion, most system parameters may vary substantially with time, especially those represented in $G(k)$. Those parameters must be identified and predicted before the optimization of the control measures $C(k)$.

A large body of dynamic prediction methods, such as time-series analysis and the Kalman filtering algorithm, which allow for performing parameter estimation and updating with the on-line surveillance data, exists in the literature. Example applications of these techniques in traffic analysis can be found elsewhere (*20,21*).

Optimization Algorithm

The above optimal control model formulated with Equations 17 through 25 is basically a nonlinear programming (NLP) problem. However, because these nonlinear constraints as well as the flow-density relation can be viewed as two connected linear functions in nature, the complex NLP becomes a series of linear programming (LP) models on alternative linear constraint regions and thus can be solved with efficient LP algorithms. To ensure that all optimal control measures can be generated in a sufficiently short time for real-time applications, a successive linear programming (SLP) algorithm was developed for this study. Step-by-step procedures for implementation follow.

SLP Algorithm

Step 1

- According to the current traffic state, $W(k-1)$, and the last control measure, $C(k-1)$, select the appropriate linear segment for use in Equations 5, 6, 9, 14, and 15
- Impose the region constraints for the equivalent LP model based on the selected segment of each two-piece function.
- Solve the LP model to produce a control solution, $C(k)$.

Step 2

Compute the resulting traffic state, $W(k)$, with this initial control measure, $C(k)$.

Step 3

Check whether any of Equations 5, 6, 9, 14, or 15 yields the identical value with either of its two functions under the projected $W(k)$ and the implemented $C(k)$. If not, this solution $C(k)$ is optimal and the search process terminates. Otherwise, go to Step 4.

Step 4

- Replace those inequality constraints for any of Equations 5, 6, 9, 14, or 15 with their complement piece of functions.
- Solve the modified LP model to generate a new $C(k)$.

Step 5

Check whether the objective function value (i.e., total throughput) has been improved after changing the constraints. If not, the current measure, $C(k)$, is the optimal solution, and the search process can be terminated. Otherwise, return to Step 2.

Discussion of SLP Algorithm

The algorithm starts with an initial LP model that is based on the current traffic state. Appropriate linear flow-density functions are then determined for Equations 5 and 6 according to the current link density. If the density is less than its critical value, ρ^{cr}, the left-segment linear function is selected; otherwise, the right-segment linear function is used. Similarly, in Equations 9, 14, and 15, the algorithm will select one of two complement functions that reduces its value with the current traffic state data. The initial LP model thus can be constructed by incorporating the boundaries of the selected linear functions (i.e., Equations 14 and 15) into its constraints.

To examine whether the initial LP formulations actually yield the optimal solution, Step 3 is taken to compare the resulting values from both of the two linear functions in Equations 5, 6, 9, 14, and 15, according to the traffic state projected in Step 2 with the initial control measure, $C(k)$. If none of the two linear functions in these equations are equal, the imposed linear constraint region contains the optimal solution, and therefore the obtained LP solution is the optimal control measure. However, very often some of the two complement linear functions may yield the same value as the given LP solution, indicating that some of the incorporated boundaries for the linear functions become binding constraints at the solution point. Apparently, the optimal control solution is not within the imposed linear region; it may lie on the boundaries or beyond the linear region. Therefore, Step 4 is executed to check whether the optimal solution point is on any of the boundaries. Through replacement of the binding inequality constraints, Step 4 and Step 5 are executed to see whether some improvement can be made. If not, the previously obtained LP solution is optimal and is located on a boundary point of the imposed linear region. The proposed algorithm repeats this procedure to successively solve a series of LP problems until the optimal control solution is reached.

The following key features make the SLP algorithm especially suitable for use in real-time implementations:

- It is convenient to implement because only LP problems need to be solved, and its formulation need not have any derivatives.
- The LP solution improves monotonically from one iteration to next.
- The algorithm often terminates within a small number of iterations and no loop may exist during the iteration process.

The SLP approach has been calibrated and tested successfully for use on an integrated real-time ramp metering control system (*22*).

Refined Real-Time Feedback Control Procedure

As indicated in Figure 4, by computing the control measures $C(k)$, the system parameters $G(k+m)$ $(m = 0, 1, \ldots, M-1)$ will all be updated and predicted with real-time surveillance data. That feedback is necessary to achieve adaptive on-line control. Such feed-

back information is critical, especially when nontrivial bias exists for previously predicted parameters.

According to the rolling time horizon logic, if the accuracy of predicted parameters is within an acceptable range, the optimization need not be executed in subsequent intervals within the time horizon. The control logic, along with the implemented rolling time horizon concept, is shown in Figure 5.

NUMERICAL EXAMPLE

To illustrate the proposed model as well as the solution algorithm for potential real-time applications, an example scenario with simulation was developed.

Simulation Tool

To evaluate the proposed real-time incident-responsive control, a traffic simulation model must be used to provide the surveillance data required by the control model. The microscopic simulation model INTRAS (*23*), developed by FHWA for freeway corridor simulation analysis, was selected for preliminary evaluation. In the numerical example, INTRAS was used to execute the control measures generated by the SLP algorithm, including on-ramp metering rates, off-ramp diversion rates, and g/C ratios for surface street signals. Interactively, the on-line surveillance data produced by INTRAS are fed back to the SLP algorithm to compute the new control measures for subsequent time intervals. The INTRAS model also provides all the most commonly used measures of effectiveness (MOEs) for evaluation.

Network and Case Design

Figure 6 shows a sample corridor network. The network consists of four identical segments. Each contains a two-lane freeway with auxiliary lanes, a three-lane arterial street, one on-ramp, one off-ramp, and one crossing surface street. All street intersections are signal controlled.

Each time interval is 3 min long. A total of 20 time intervals were used in the INTRAS simulation runs. An incident was assumed to occur on the downstream end of the second segment from time intervals 3 to 8. A detailed description of the experimental design and its implementation on INTRAS can be found elsewhere (*24*).

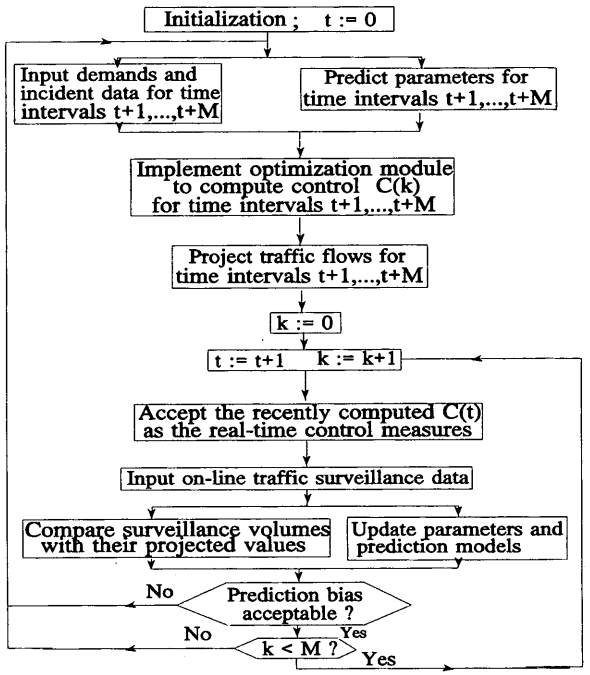

FIGURE 5 Refined real-time feedback control logic.

The following three cases with different freeway traffic loadings were simulated in the experiment: Case 1, high freeway demand (3,300 vph) with a severe incident (50 percent reduction in capacity); Case 2, moderate freeway demand (3,000 vph) with a severe incident (50 percent reduction in capacity); and Case 3, low freeway demand (2,600 vph) with a minor incident (25 percent reduction in capacity).

On surface streets, an entry volume of 1,200 vph is assumed at the upstream control boundary of the arterial street. On each crossing street, the entry flow is assumed to be maintained at 600 vph, with 30 percent of vehicles turning right to the arterial street. For evaluation of the model's effectiveness, four scenarios were developed for each case: (*a*) no control, (*b*) on-line strategy produced by the proposed model, (*c*) moderate control (Control A), and (*d*) intensive control (Control B). Control A and Control B for each case are briefly described:

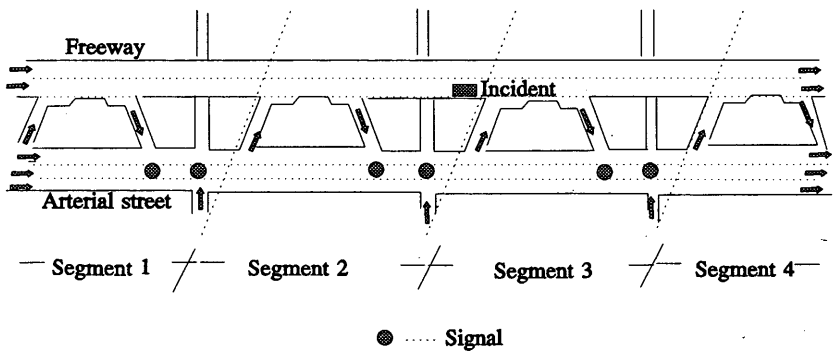

FIGURE 6 Corridor network example.

TABLE 2 Total Throughput from Simulation Results

Scenarios	Case 1		Case 2		Case 3	
	throughput	throughput increase	throughput	throughput increase	throughput	throughput increase
No control	6893	0	6616	0	6192	0
Control -A	6936	43	6624	8	6240	48
Control -B	6936	43	6610	0	6259	67
On-line control	7218	325	6849	233	6605	413

- Case 1: Control A is a moderate diversion control, whereby the first two on-ramps are closed and 10 percent of freeway vehicles are assumed to divert via the off-ramps of the first two corridor segments. The g/C ratio of traffic signals is adjusted accordingly to respond to the diverting traffic. For the intensive control case, Control B, 20 percent of freeway traffic will divert at the second two subsequent off-ramps.
- Case 2: Control A represents a moderate diversion control under which the first two on-ramps are closed and 10 percent of freeway traffic will divert via the second off-ramp. The g/C ratio of traffic signals is adjusted accordingly to respond to the diverting traffic. For the intensive control case, Control B, 20 percent of freeway traffic will divert at the second off-ramp.
- Case 3: Because of the light freeway traffic demand and the minor incident involved, only the second on-ramp will be closed for Control A. As for Control B, in addition to the ramp closure, 5 percent of freeway traffic will divert at the second off-ramp. The g/C ratios of traffic signals are adjusted to respond to the diverting traffic.

All diverted freeway traffic is assumed to reenter the freeway at the nearest downstream on-ramp beyond the incident, if the on-ramp capacity allows. If the nearest on-ramp reaches its capacity, diverted traffic will proceed on the surface street and reenter the freeway via the next available on-ramp. Note that neither Control A nor Control B, in any case, was randomly selected for evaluation. Each actually represents a reasonable control plan produced by senior freeway operation engineers. In addition, g/C ratios of all traffic signals are adjusted or optimized on the basis of expected diverting traffic patterns.

Simulation Results

Although a wide variety of MOEs, including total vehicle-miles, total vehicle-minutes, average travel speed, and total delay, are available in the output of INTRAS, most of them have some limitations for use in guiding real-time corridor control. For instance, high vehicle-miles may be accompanied by high vehicle-minutes or a low average speed. Similarly, the objective of maximizing speed or minimizing total delay may imply fewer vehicles being served. Therefore, total corridor throughput remains a more reasonable MOE for evaluation. Table 2 indicates the total corridor throughput resulting from the simulation runs for all cases and scenarios.

It is evident that the proposed on-line control algorithm produced the highest total corridor throughput in all cases (Table 2).

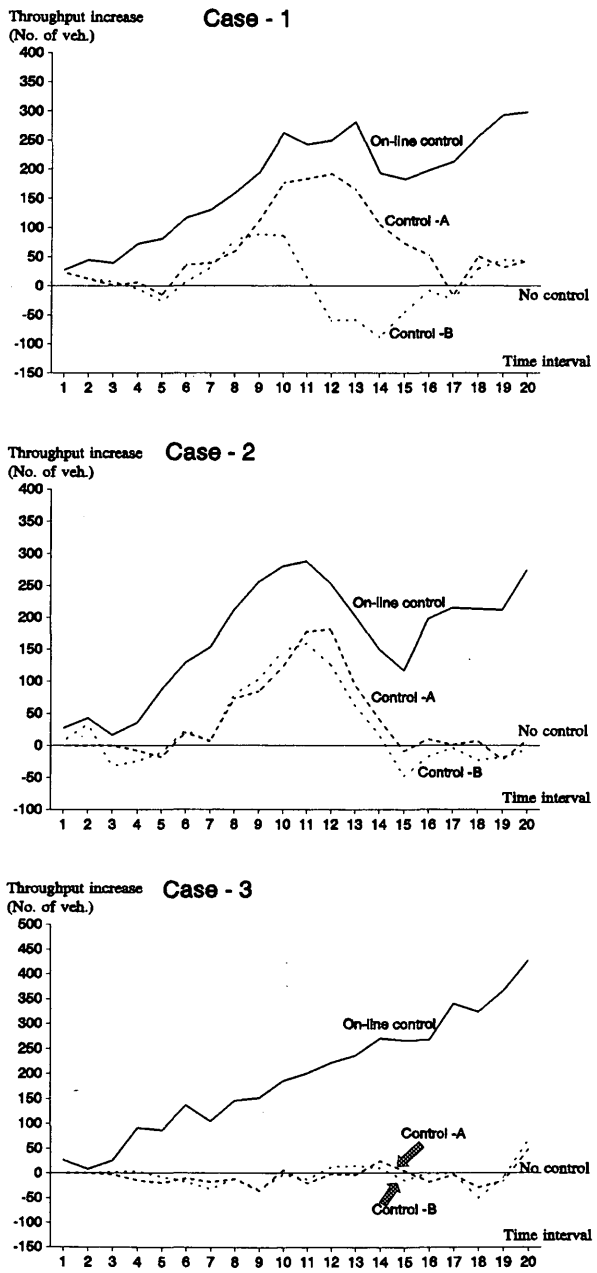

FIGURE 7 Cumulative throughput increase versus no control.

"Throughput increase" in Table 2 denotes the total corridor throughput increases for each scenario compared with the no-control scenario at the end of the 60-min control period. To better demonstrate the superior performance of the proposed approach, the time-varying cumulative throughput increase for 20 time intervals in four control scenarios is presented in Figure 7, for the three illustrative cases. Except for Case 3 (low freeway traffic demand with a minor incident) and Control B of Case 1, all control scenarios produce higher corridor throughput than the no-control case during the incident period. Among the four scenarios, the on-line control performs best during the entire control period.

CONCLUSIONS

A modeling framework, as well as formulations for its use for real-time freeway incident control, was presented. The proposed model is capable of generating the optimal control target for all available control measures, including on-ramp metering rates, off-ramp diversion fractions, and signal timing plans at surface street intersections in an entire corridor. By approximating the nonlinear flow-density relation with two linear complement functions, the study developed an efficient algorithm, named SLP, to solve the proposed integrated freeway diversion control model. Preliminary results from the numerical example with INTRAS have demonstrated the potential efficacy of the proposed modeling system as well as algorithm.

Further research along this line, conducted at the University of Maryland, incorporates an advanced signal control at surface intersections and extension of control boundaries to multiple surface streets. Thus, both freeways and surface street networks can be operated under a consistent control strategy.

REFERENCES

1. Cremer, M., and S. Schoof. On Control Strategies for Urban Traffic Corridors. In *Proceedings of IFAC Control, Computers, Communications in Transportation,* Paris, 1989.
2. Cremer, M., and S. Fleischmann. Traffic Responsive Control of Freeway Networks by a State Feedback Control. In *Transportation and Traffic Theory* (Gartner and Wilson, eds.), Elsevier, New York, 1987, pp. 213–219.
3. Chang, G.-L., P.-K. Ho, and C.-H. Wei. A Dynamic System-Optimal Control Model for Commuting Traffic Corridors. *Transportation Research C,* Vol. 1C, pp. 1–12.
4. Gartner, N. H., and R. A. Reiss. Congestion Control in Freeway Corridors: The IMIS System. In *Flow Control of Congested Networks* (A. R. Odoni et. al., eds.), Springer-Verlag, 1987.
5. Reiss, R. A., et al. Development of Traffic Logic for Optimizing Traffic Flow in an Intercity Corridor. Final report. U.S. Department of Transportation, 1978.
6. Reiss, R. A., et al. Algorithm Development for Corridor Traffic Control. In *Traffic, Transportation, and Urban Planning* (Vol. 2), George Goodwin, London, 1981.
7. Reiss, R. A., N. H. Gartner, and S. L. Cohen. Dynamic Control and Traffic Performance in a Freeway Corridor: A Simulation Study. *Transportation Research A,* Vol. 25A, 1991, pp. 267–276.
8. Goldstain, N. B., and K. S. P. Kumar. A Decentralized Control Strategy for Freeway Regulation. *Transportation Research B,* Vol. 16B, 1982, pp. 279–290.
9. Papageorgiou, M. A New Approach to Time-of-Day Control Based on a Dynamic Freeway Traffic Model. *Transportation Research B,* Vol. 14B, 1980, pp. 349–360.
10. Papageorgiou, M. A Hierarchical Control System for Freeway Traffic. *IEEE Transactions on Automatic Control,* Vol. AC-29, 1983, pp. 482–490.
11. Papageorgiou, M., J.-M. Blosseville, and H. Hadj-Salem. Modeling and Real Time Control of Traffic Flow on the Southern Part of Boulevard Peripherique in Paris; Part II: Coordinated On-Ramp Metering. *Transportation Research A,* Vol. 24A, 1990, pp. 361–370.
12. Payne, H. J., D. Brown, and J. Todd. *Demand Responsive Strategies for Interconnected Freeway Ramp Control Systems,* Vol. 1: Metering Strategies. Verac Inc., 1985.
13. Hall, F. L. Empirical Analysis of Freeway Flow-Density Relationships. *Transportation Research A,* Vol. 20A, 1986, pp. 197–210.
14. Banks, J. H. Freeway Speed-Flow-Concentration Relationships: More Evidence and Interpretations. In *Transportation Research Record 1225,* TRB, National Research Council, Washington D.C., 1989, pp. 53–60.
15. Robertson D. I. *TRANSYT: A Traffic Network Study Tool.* Road Research Laboratory Report LR253, Crowthorne, England, 1969.
16. Axhausen, K. W., and H.-G. Körling. Some Measurements of Robertson's Platoon Dispersion Factor. In *Transportation Research Record 1112,* TRB, National Research Council, Washington D.C., 1987, pp. 71–77.
17. Boillot, F., et al. Optimal Signal Control of Urban Traffic Networks. *Proc. 6th International Conference on Road Traffic Monitoring and Control,* IEE, London, 1992.
18. Gartner, N. H. OPAC: A Demand-Responsive Strategy for Traffic Signal Control. In *Transportation Research Record 906,* TRB, National Research Council, Washington D.C., 1983, pp. 75–80.
19. Henry, J. J., et al. The PRODYN Real Time Traffic Algorithm. *Proc., 4th IFAC-IFIP-IFORS Conference on Control in Transportation Systems,* Baden-Baden, Germany, 1983.
20. Lu, J. Prediction of Traffic Flow by an Adaptive Prediction System. In *Transportation Research Record 1287,* TRB, National Research Council, Washington D.C., 1991, pp. 54–61.
21. Stephanedes, Y. J., E. Kwon, and P. Michalopoulos. On-Line Diversion Prediction for Dynamic Control and Vehicle Guidance in Freeway Corridors. In *Transportation Research Record 1287,* TRB, National Research Council, Washington D.C., 1991, pp. 11–19.
22. Wu, J. *Development and Evaluation of Real-Time Ramp Metering Algorithms.* FHWA, U.S. Department of Transportation, 1993.
23. Wicks, D. A., and E. B. Lieberman. *Developing and Testing of INTRAS, a Microscopic Freeway Simulation Model.* Report FHWA/RD-80/106-109, Vol. 1–4, FHWA, U.S. Department of Transportation, 1980.
24. Lieu, H. C. *An Integrated Diversion Control System for Freeway Corridors.* Ph.D Dissertation. Department of Civil Engineering, University of Maryland, College Park, 1993.

Publication of this paper sponsored by Committee on Transportation Supply Analysis.